ARTICLE
Journal of Cellular Biochemistry 115:959–966 (2014)

Journal of Cellular Biochemistry

OA10 Is a Novel p38alpha Mitogen-Activated Protein Kinase Inhibitor That Suppresses Osteoclast Differentiation and Bone Resorption

T. Jiang,[1] A. Qin,[2,3] Z.Y. Shao,[4] B. Tian,[3] Z.J. Zhai,[3] H.W. Li,[3] Z.A. Zhu,[3] K.R. Dai,[3] H. Zheng Ming,[2] Y.P. Yu,[4**] and Q. Jiang[1*]

[1]*The Center of Diagnosis and Treatment for Joint Disease, Drum Tower Clinical Medical College of Nanjing Medical University, Jiangsu, P.R. China*

[2]*Centre for Orthopaedic Research, School of Surgery, The University of Western Australia, Perth, Australia*

[3]*Shanghai Key Laboratory of Orthopaedic Implants, Department of Orthopaedics, Ninth People's Hospital, Shanghai Jiao Tong University School of Medicine, Shanghai, P.R. China*

[4]*College of Pharmaceutical Sciences, Zhejiang University, Hangzhou, P.R. China*

ABSTRACT

In search of anti-bone resorbing agents for the potential treatment of osteoporosis, we synthesized a novel compound Tert-butyl 4-(3-[1H-indole-2-carboxamido]benzoyl)piperazine-1-carboxylate (OA10) and found that OA10 is capable of inhibiting RANKL-mediated osteoclast formation and osteoclastic bone resorption in a dose-dependent manner. This biological effect is further supported by the fact that OA10 suppressed osteoclastic-specific gene expression, including tartrate-resistant acid phosphatase, cathepsin K receptor, and calcitonin receptor. Further molecular mechanism investigation revealed OA10 inhibited p38 phosphorylation, suppressed c-fos and NFATc1 expression without affecting NF-κB or JNK signaling pathways. Taken together, this study suggested that OA10 can inhibit osteoclastogenesis by suppressing p38-c-Fos-NFATc1 cascade. OA10 may be developed as a therapeutic drug for osteoclast-related osteolytic diseases. J. Cell. Biochem. 115: 959–966, 2014.

KEY WORDS: O10; OSTEOCLAST DIFFERENTIATION; p38alpha; c-Fos-NFATc1

Bone homeostasis is maintained through a subtle balance between osteoblastic bone formation and osteoclastic bone resorption. Decreased osteoblastic bone formation and/or increased osteoclastic bone resorption can lead to a variety of bone diseases such as osteoporosis, osteoarthritis, implant failure, etc. [Teitelbaum, 2000]. Therefore, current therapeutic strategies for treating these bone diseases mainly focus on identifying compounds that can enhance osteoblast bone formation or suppress osteoclast bone resorption [Simic et al., 2006].

Abbreviations: CCK-8, cell counting kit-8; FBS, fetal bovine serum; GAPDH, glyceraldehyde-3-phosphate dehydrogenase; IκBα, I-kappa-B-alpha; JNKs, c-Jun N-terminal kinases; MAPK, mitogen-activated protein kinases; M-CSF, macrophage colony-stimulating factor; MITF, microphthalmia transcription factor; MKK, MAPK kinase; NFATc1, nuclear factor of activated T-cells,1; NF-κB, nuclear factor-kappa B; RANK, receptor activator of NF-κB; RANKL, receptor activator of NF-κB ligand; SDS, sodium dodecyl sulfate; TRAP, tartrate-resistant acid phosphatase; CTSK, cathepsin K receptor; CTR, calcitonin receptor; TRAF6, tumor necrosis factor receptor-associated factor 6.

Jiang, Qin, and Shao have contributed equally to this work.

Grant sponsor: National Nature Science Foundation of China; Grant numbers: 81101338, 81125013; Grant sponsor: National Health and Medical Research Council; Grant number: 1010420; Grant sponsor: Shanghai Municipal Education Commission; Grant number: 13YZ031; Grant sponsor: National Natural Science Foundation for the Youth of China; Grant number: 81201364.

* Correspondence to: Q. Jiang, The Center of Diagnosis and Treatment for Joint Disease, Drum Tower Clinical Medical College of Nanjing Medical University, Zhongshan Road 321, Nanjing, Jiangsu 210008, P.R. China. E-mail: jiangqing112@hotmail.com

** Correspondence to: Y.P. Yu, College of Pharmaceutical Sciences, Zhejiang University, 866 Yuhangtang Road, Hangzhou, Zhejiang Province 310058, P.R. China. E-mail: yyu@zju.edu.cn

Manuscript Received: 3 December 2013; Manuscript Accepted: 5 December 2013

Accepted manuscript online in Wiley Online Library (wileyonlinelibrary.com): 19 December 2013

DOI 10.1002/jcb.24744 • © 2013 Wiley Periodicals, Inc.

Osteoclasts are multinucleated cells derived from hematopoietic stem cells. The differentiation of osteoclast is dependent on a key molecular, receptor activator of nuclear factor (NF)-κB ligand (RANKL) which is expressed by stromal cells, osteoblasts, osteocytes, and vascular endothelial cells [Chambers, 2000; Nakashima et al., 2011; Xiong et al., 2011]. The binding of RANKL to its receptor RANK on the surface of osteoclast precursor cells will initiate the activation of tumor necrosis factor receptor-associated factor 6 (TRAF6), resulting in the subsequent activation of multiple signaling cascades including NF-κB, c-Jun N-terminal kinase (JNK), p38, extracellular signal-regulated kinase (ERK), and Src signaling pathways [Grigoriadis et al., 1994; Boyce et al., 1999; Mansky et al., 2002; Gingery et al., 2003; Izawa et al., 2012]. Among them, the protein kinase p38 is particularly important in the early stages of osteoclast differentiation as p38 MAP kinases activate the critical transcription factors including c-Fos and NFATc1 that are essential for osteoclast differentiation [Matsuo et al., 2004; Tanos et al., 2005].

Based on the understanding of these key signaling pathways during osteoclast differentiation, our lab has long-term interests on synthesizing and screening novel compounds that are capable of inhibiting osteoclast formation/function [Qin et al., 2012; Li et al., 2013]. In this study, we reported the synthesis of a novel compound Tert-butyl 4-(3-[1H-indole-2-carboxamido]benzoyl) piperazine-1-carboxylate (termed as OA10) that is capable of inhibiting osteoclast formation by modulation of p38 signaling pathway.

MATERIALS AND METHODS

REAGENTS AND ANTIBODIES

RAW264.7 cells were obtained from the American Type Culture Collection (Rockville, MD). TRAP staining solution was from Sigma–Aldrich (St. Louis, MO). Soluble human recombinant macrophage-colony-stimulating factor M-CSF and bacteria-derived recombinant mouse RANKL were purchased from R&D (R&D Systems, Minneapolis, MN). Antibodies against c-Fos, NFATc1, and GAPDH were obtained from Santa Cruz Biotechnology, Inc. (Santa Cruz, CA). Antibodies against phospho-ERK, ERK, phospho-JNK, JNK, phospho-p38, p38, phospho-IκB, and IκB were from Cell Signaling Technology (Danvers, MA).

BMM ISOLATION OSTEOCLAST DIFFERENTIATION AND TRAP STAINING

Mouse bone marrow cells were obtained from femurs and tibiae of a 4-week-old C57BL/6 mouse and were maintained in α-MEM complete media supplemented with 10% fetal bovine serum (FBS; Gibco BRL, Gaithersburg, MD), 100 U/ml penicillin in a T 75 in the presence of M-CSF (30 ng/ml) for 3 days. Adherent cells on T75 bottoms were classified as bone marrow macrophages (BMMs). BMMs (7×10^3 cells/well) were cultured in complete medium in the presence of M-CSF (30 ng/ml) and RANKL (50 ng/ml) in a 96-well (100 μl/well) plate with OA10 at varying concentrations (0, 0.3125, 0.625, and 1.25 μM). After 4 days, cells were fixed with 4% paraformaldehyde for 20 min, washed with PBS, and then stained with tartrate-resistant acid phosphatase (TRAP) using the Leukocyte Acid Phosphatase Assay Kit (Sigma–Aldrich). TRAP-positive multinucleated cells were counted as osteoclast-like cells.

CYTOTOXICITY ASSAYS

Cell Counting Kit-8 (Dojindo Molecular Technology, Japan) is used in the measurement of cytotoxicity according to the manufacturer's instructions. BMMs (7×10^3 cells/well) were cultured with OA10 at various concentrations (0, 0.078, 0.156, 0.3125, 0.625, 1.25, 2.5, and 5 μM) for 48 h in the presence of M-CSF (30 ng/ml) in 96-well plates (100 μl/well). After a 3-h incubation, cells in a medium containing 10 μl of CCK-8 solution, OD was read as 450 nm (650 nm reference) using 96-well plate reader. The half-maximal inhibitory concentration (IC_{50}) value was calculated by GraphPad Prism program version 5.0c (San Diego, CA).

BONE RESORPTION ASSAY

BMMs were seeded in a collagen gel matrix-coated 90-mm dish induced by RANKL (50 ng/ml), M-CSF (30 ng/ml) until the formation of mature osteoclast cells. Then, the osteoclasts were digested by collagenase and seeded onto bovine bone slices in a 96-well plate with RANKL (100 ng/ml), M-CSF (30 ng/ml), and OA10 (0, 0.625, 1.25, and 2.5 μM) for 48 h. After osteoclast-like (OCL) cells were observed, the OCL cells were removed from bone slices by mechanical agitation and sonication. The resorption pits were photographed under a scanning electron microscope (SEM, FEI Quanta 250). Total resorption pit areas were quantified using the ImageJ software (National Institutes of Health).

RNA EXTRACTION AND QUANTITATIVE PCR ANALYSIS

Total RNA was prepared using the Qiagen RNeasy Mini kit (Qiagen, Victoria, Australia) according to the manufacturer's instructions, and cDNA was synthesized from 2 μg of total RNA using the iScript cDNA Synthesis Kit (Bio-Rad, Hercules, CA). Then, real-time PCR was performed on an ABI 7500 Sequencing Detection System using the SYBR Premix Ex Taq™ II. Briefly, 5 μl of SYBR Premix Ex Taq™ II, 2.8 μl ddH_2O, 0.4 μl cDNA, 0.2 μl Dye II, and 0.8 μl of each primer were mixed to make up a total volume of 10 μl for each PCR. The detector was programmed with the following PCR conditions: 40 cycles for 5 s denaturation at 95°C and 34 s amplification at 60°C. β-actin was included as housekeeping gene and all reactions were run in triplicates. T. Relative differences in PCR results were evaluated comparative $2^{-\Delta\Delta CT}$ method. The specific primer sequences were used: mouse c-Fos, 5′-CTGGTGCAGCCCACTCTGGTC-3′ (forward) and 5′-CTTTCAGCAGATTGGCAATCTC-3′ (reverse); NFATc1, 5′-CTCGAAAGACAGCACTGGAGCAT-3′ (forward) and 5′-CGGCTGCCTTCCGTCTCATAG-3′ (reverse); TRAP, 5′-CTGGAGTGCACGATGCCAGCGACA-3′ (forward) and 5′-TCCGTGCTCGGCGATGGACCAGA-3′ (reverse); cathepsin K, 5′-CTTCCAATACGTGCAGCAGA-3′ (forward) and 5′-TCTTCAGGGCTTTCTCGTTC-3′ (reverse); calcitonin receptor (CTR), 5′-TGCAGACAACTCTTGGTTGG-3′ (forward) and 5′-TCGGTTTCTTCTCCTCTGGA-3′ (reverse) [Feng et al., 2009; Qin et al., 2011]; and β-actin, 5′-AGCGGGAAATCGTGCGTG-3′ (forward) and 5′-CAGGGTACATGGTGCC-3′ (reverse).

WESTERN BLOT ANALYSIS

Raw264.7 cells were seeded in 6-well plate pretreated with vehicle or OA10 (2.5 μM) for 2 h. Subsequently, stimulated with RANKL for 0, 5, 10, 20, 30, and 60 min. BMMs were cultured with OA10 (0 and 2.5 μM) in the presence of MCSF (30 ng/ml) and RANKL (50 ng/ml) for 5 days. The cells were lysed in a buffer containing 50 mM Tris pH 7.5, 150 mM

NaCl, 1% Nonidet161 P-40, 1% sodium deoxycholate, 0.1% SDS included with PMSF (Shen Neng Bo Cai Corp. China). The lysate was shaken up on ice for 20 min and centrifuged at 12,000 rpm for 10 min and the protein concentration in the supernatant was measured with BCA protein assay kit (Thermo Scientific, Rockford). Equal amounts of proteins were separated using 8–10% sodium dodecyl sulfate-polyacrylamide gel electrophoresis (SDS–PAGE) and were transferred to PVDF membranes (Roche). The membranes were blocked with 5% skim milk for 1 h and were then probed with the appropriate primary antibodies at room temperature for 4 h. Accordingly horseradish peroxidase-conjugated secondary antibodies (1:5,000) were incubated to the membranes for 1 h. Finally, the immunoreactivity was detected by exposure in an Odyssey infrared imaging system.

STATISTICAL ANALYSIS

All the results are expressed as the mean ± SD from at least three independent experiments. Statistical difference was determined by Student's *t*-test. Significance was considered at $^{*}P < 0.05$ or $^{**}P < 0.01$.

RESULTS

SYNTHESIS OF OA10

The compound OA10 was synthesized as shown in Figure 1A. In brief, 3-aminobenzoic acid (15.0 mmol) was dissolved in methanol (15.0 ml), then 98% H_2SO_4 (2.0 ml) was slowly added to the mixture. After stirring at 60°C for 6 h, the reaction was cooled down to room temperature. The mixture was reduced to 5.0 ml by rotary evaporation. The reaction mixture was neutralized by 25.0 ml saturated aqueous sodium bicarbonate solution. The isolated yield after extraction with ethylacetate (15.0 ml × 3) and rotary evaporation in vacuo was 95% for 2. 1H-indole-2-carboxylic acid (1) (10.0 mmol) and methyl 3-aminobenzoate (2) were dissolved in 30.0 ml CH_2Cl_2. The mixture was been stirring for 12 h at 30°C in the presence of 20.0 mmol EDCI, 20.0 mmol HOBt, and 20.0 mmol Et_3N. After the reaction was finished, the mixture was washed by 30.0 ml saturated $NaHCO_3$ (aq.) and 30.0 ml water. The organic layer was rotary evaporated after it was dried by Na_2SO_4. The corresponding product was obtained in high yield (90% for 3) via recrystallization (ethyl acetate/n-hexane, 3:1; 15.0 ml). Treating methyl 3-(1H-indole-2-carboxamido)-benzoate (3) (7.0 mmol) with 1 M NaOH (aq.) (15.0 ml) for 4 h. After the reaction was finished, the solution was rotary evaporated to one-third of its original volume. 3-(1H-indole-2-carboxamido) benzoic acid (4) was isolated via filtration after 3 M hydrochloric acid (10.0 ml) was slowly added to the mixture at 0°C. N-(3-[piperazine-1-carbonyl] phenyl)-1H-indole-2-carboxamide (5) was synthesized by condensation of 3-(1H-indole-2-carboxamido) benzoic acid (4) (5.0 mmol) with 5.0 mmol of piperazine in the presence of 10.0 mmol EDCI, 10.0 mmol HOBt, and 10.0 mmol Et_3N in CH_2Cl_2 at 30°C for 12 h. Product was obtained as white solid after column chromatography (silica/DCM-MeOH, up to 5% MeOH) in good yield (60% for 5). The compound was fully characterized and confirmed by ^{1}H NMR, ^{13}C NMR, and HRMS (ESI positive).

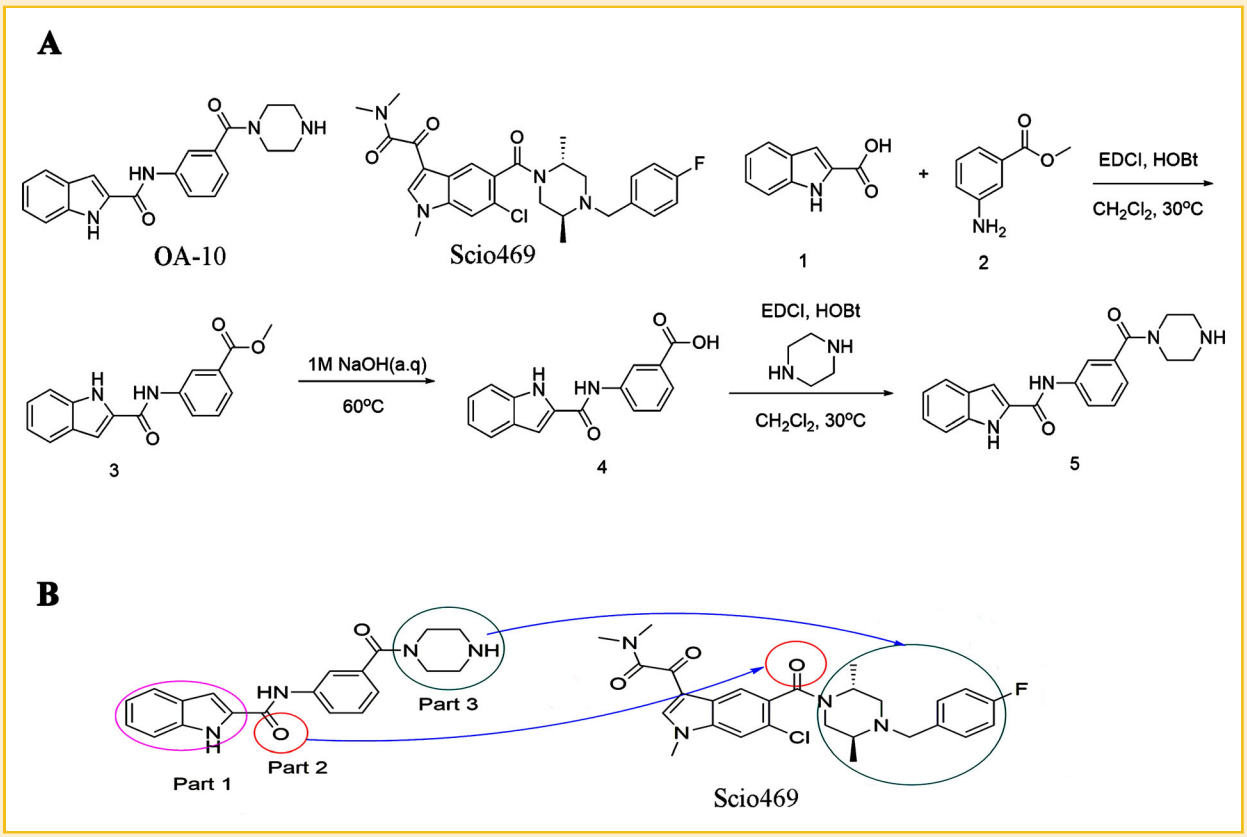

Fig. 1. A: Chemical structure of OA10; synthesis of OA-4 (includes chemical structures). B: The relationship between OA10 and Scio469.

^{1}H NMR (500 MHz, DMSO-d_6) δ 11.79 (s, 1H), 10.37 (s, 1H), 8.00–7.79 (m, 2H), 7.67 (d, J = 8.0 Hz, 1H), 7.46–7.41 (m, 3H), 7.26–7.02 (m, 3H), 3.53 (m, 8H), 2.78 (s, 1H). ^{13}C NMR (125 MHz, DMSO-d_6) δ 168.80 (s), 159.34 (s), 138.06 (s), 136.00 (s), 128.52 (s), 128.09 (s), 127.60 (s), 127.07 (s), 125.36 (s), 124.35 (s), 122.45 (s), 122.14 (s), 120.85 (s), 111.47 (s), 110.83 (s), 45.62 (s), 45.04 (s). HRMS (ESI) m/z calcd for $C_{20}H_{20}N_4O_2$ $[M+H]^+$: 349.1659. Found: 349.1662.

OA10 INHIBITS RANKL-INDUCED OSTEOCLAST DIFFERENTIATION

In order to investigate the effect of OA10 on osteoclastogenesis, bone marrow derived monocytes/macrophages (BMMs) were cultured in the presence of M-CSF (30 ng/ml) and RANKL (50 ng/ml) without or with different concentration of OA10. In the control group, BMMs differentiated into characteristic TRAP-positive multinucleated osteoclasts. In contrast, the formation of TRAP-positive multinucleated osteoclasts was significantly suppressed after OA10 treatment, evidenced by reduced osteoclast size and number (Fig. 2A). There are about 80 osteoclasts formed per well in the control group. On the contrary, the number of osteoclast formed in the OA10 treated group decreased in a dose-dependent manner, with approximately 60, 40, and 20 osteoclasts formed after being treated with OA at 0.3125, 0.625, and 1.25 μM, respectively (Fig. 2A). In the meantime, the size of osteoclast is also reduced in the similar range (Fig. 2A). In order to eliminate the possibility that the reduction in osteoclasts formation was due to cell cytotoxicity, the cytotoxicity of OA10 on BMMs was tested. As shown in Figure 2B, the IC_{50} value of OA10 was approximately 3.614 μM. Given the fact that OA10 at concentration as low as 0.3125 μM effectively suppressed osteoclastogenesis but had no cytotoxicity on BMMs, it suggested that OA10 inhibited osteoclast differentiation without major cytotoxic effects on osteoclast precursor cells.

OA10 SUPPRESSED OSTEOCLAST-SPECIFIC GENE EXPRESSION

To further elucidate the role of OA10 on osteoclast differentiation, we examined the effects of OA10 on the expression of the osteoclastic-specific marker genes. As shown in Figure 3A, mature osteoclast-specific genes including TRAP, cathepsin K receptor (CTSK), and CTR were significantly upregulated during osteoclast differentiation.

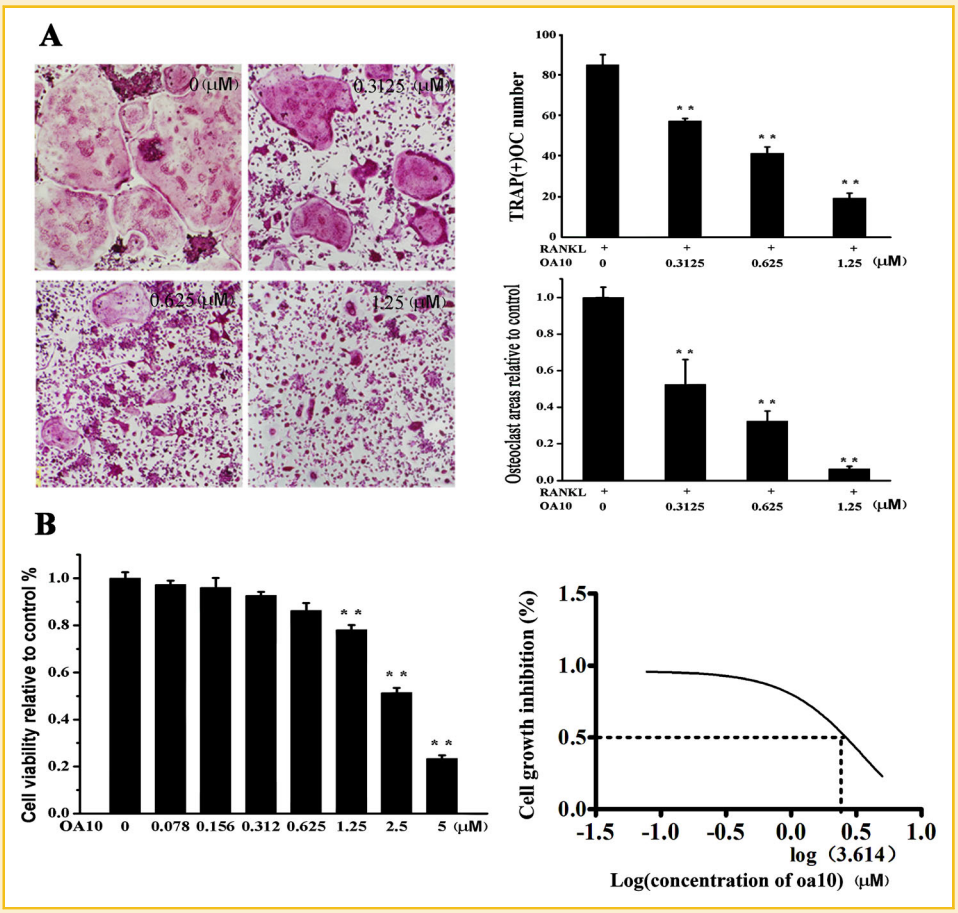

Fig. 2. OA10 inhibits RANKL-induced osteoclastogenesis. A: BMMs were cultured with the indicated concentrations of OA10. After 4 days, the cells were fixed with 4% paraformaldehyde and subjected to TRAP staining (left). The number of TRAP-positive, multinucleated (>3 nuclei) osteoclasts was counted as osteoclast-like (OCL) cells (right) ($^{*}P<0.05$; $^{**}P<0.01$). B: BMMs were cultured in complete α-MEM medium and the indicated concentrations of OA10 for 48 h. The cell viability relative to control was measured using CCK-8 reagent (left). The inhibition rate of BMMs was calculated using GraphPad Prism software, and the half-maximal inhibitory concentration (IC50) was 3.614 μM (right) ($^{*}P<0.05$; $^{**}P<0.01$).

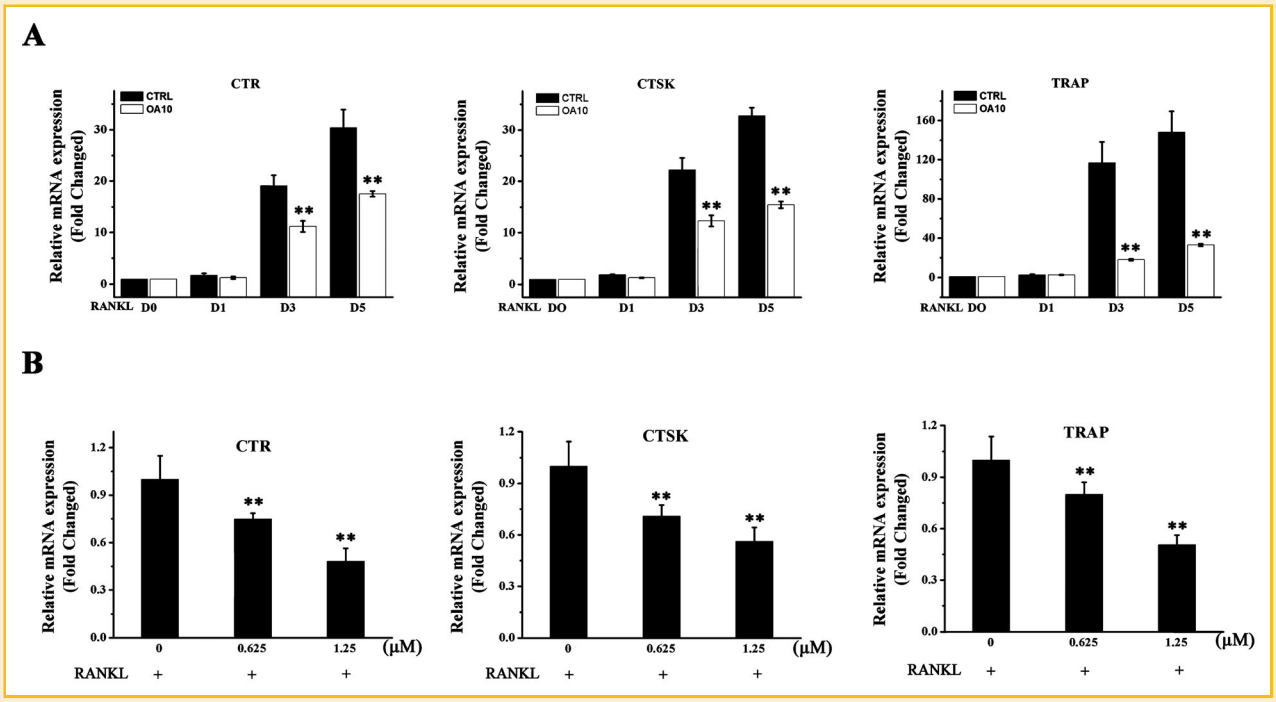

Fig. 3. OA10 suppressed RANKL-induced gene expression. BMMs were cultured with MCSF (30 ng/ml), RANKL (50 ng/ml) and the 1.25 μM OA10 (A) for 0, 1, 3, and 5 days or with M-CSF (30 ng/ml), RANKL (50 ng/ml) and indicated concentrations of OA10 for 5 days (B). RANKL-induced osteoclast-specific gene expressions were analyzed by real-time PCR. RNA expression level was normalized relative to the expression of β-actin ($^{*}P < 0.05$; $^{**}P < 0.01$).

However, the expression of these marker genes was suppressed by the addition of OA10 during osteoclastogenesis. In accordance with these results, treatment with OA10 also suppressed osteoclast-specific gene expression in a dose-dependent manner (Fig. 3B). Collectively, these results suggested that OA10 attenuated osteoclastic gene expression during osteoclastogenesis.

OA10 IMPAIRED OSTEOCLASTIC BONE RESORPTION

Based on the fact that OA10 inhibited osteoclast differentiation in vitro, it is expected that OA10 might serve as an anti-resorptive compound for potential treatment of bone diseases. Thus, we further examined the anti-resorptive effect of OA10 on osteoclasts. As shown in Figure 4A, osteoclasts without OA10 treatment actively resorbed the bone matrix.

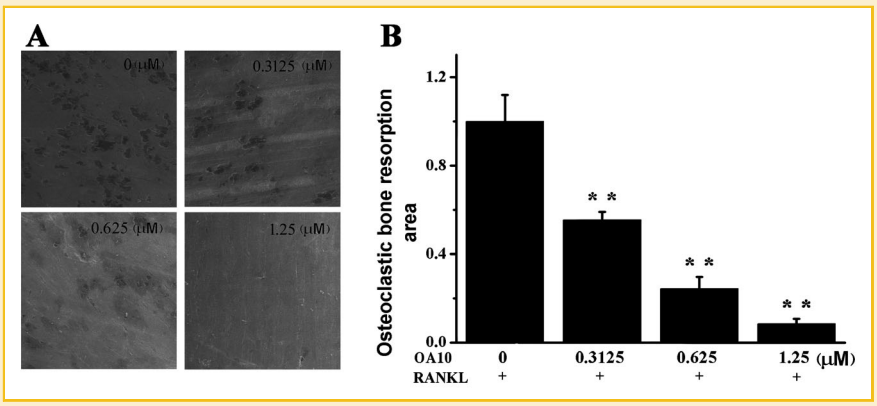

Fig. 4. OA10 attenuated osteoclastic bone resorption in vitro. Equal number of osteoclasts were seeded onto bone slices and allowed to adhere to the surface with the treatment of M-CSF (30 ng/ml), RANKL (50 ng/ml), and OA10 at varying doses (0, 0.312, 0.625, and 1.25 μM). A: Representative SEM images of bone resorption pits are shown. B: The total areas of resorption pits were measured using ImageJ and are shown graphically. Similar results were obtained from at least three independent experiments ($^{*}P < 0.05$; $^{**}P < 0.01$).

In contrast, more than 40% of bone resorption activity was attenuated by OA10 at 0.3125 μM. Surprisingly, the bone resorption activity was almost entirely blocked by OA10 at 1.25 μM, the concentration that suppressed approximately 80% of osteoclast formation. Quantitative analysis of the bone resorption area confirmed that OA10 impaired osteoclast bone resorption in a dose-dependent manner (Fig. 4B). Taken together, these results indicated that OA10 dose dependently impaired the bone resorption activity of mature osteoclasts.

OA10 SUPPRESSED RANKL-INDUCED PHOSPHORYLATION OF P38 SIGNALING PATHWAY

To further investigate the molecular mechanisms underlying the inhibitory effects of OA10 on osteoclast formation and function, RANKL-induced signaling cascades, including p38 phosphorylation, JNK phosphorylation, and IκBα degradation were examined. As shown in Figure 5A, p38 phosphorylation was activated by RANKL stimulation from 5 min and sustained until 20 min. Meanwhile, the phosphorylation of p38 was significantly suppressed by OA10 at 1.25 μM. In addition, it was interesting to note that JNK phosphorylation and IκBα degradation were not affected after OA10 treatment. Taken together, these results suggested OA10 suppressed the phosphorylation of p38 without affecting JNK or IκBα activation.

During the course of osteoclastogenesis, the RANKL-induced phosphorylation of p38 subsequently activated the inchoate and terminal transcription factors, c-Fos and NFATc1, respectively

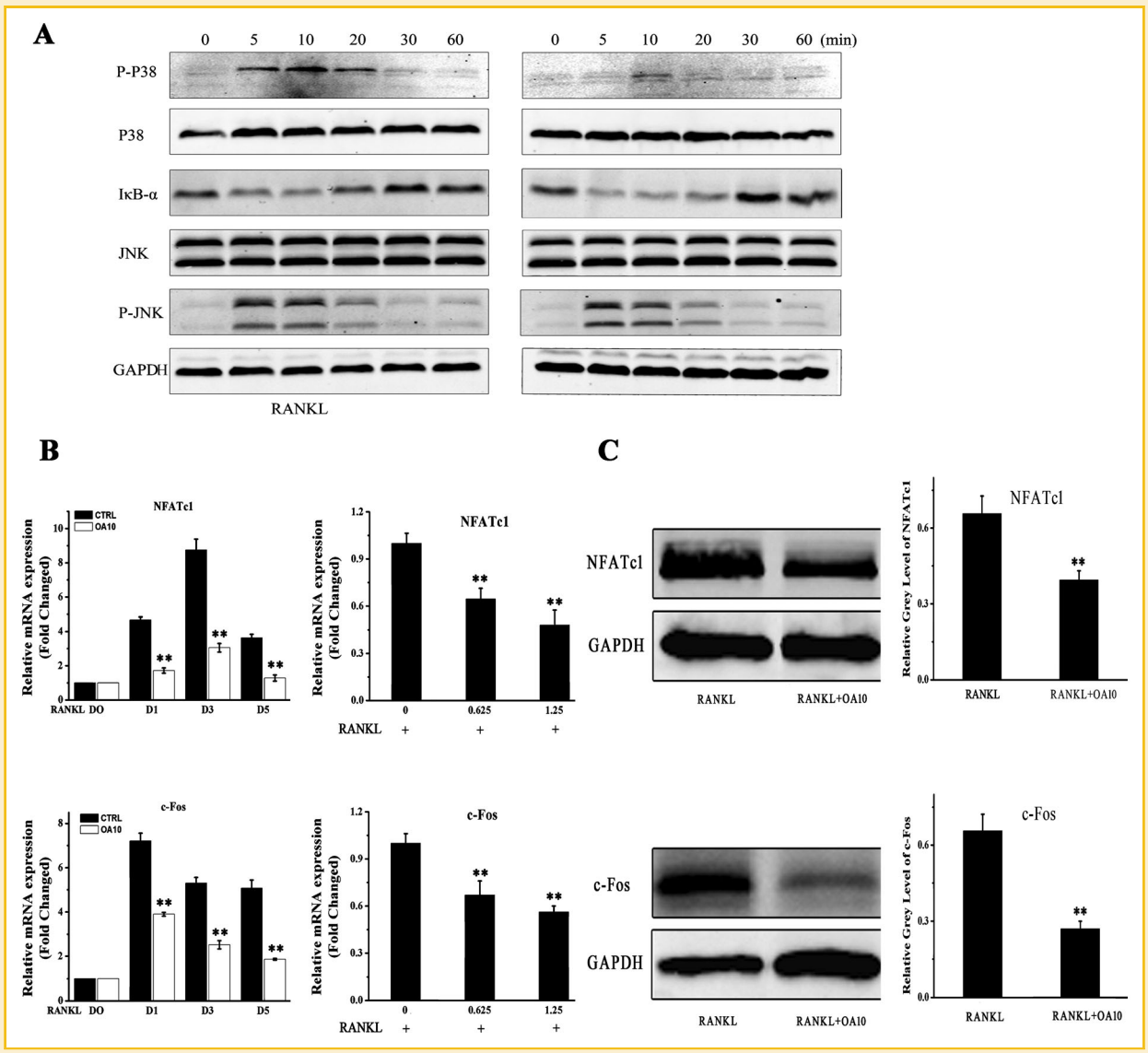

Fig. 5. A: OA10 inhibits the RANKL-induced phosphorylation of p38. RAW264.7 cells were pretreated with vehicle or OA10 for 2 h followed by RANKL stimulation (50 ng/ml) for the indicated times period. Then lysates were in lysis buffer, and protein expression levels were analyzed by Western blotting with the indicated antibodies (top). B: OA10 suppressed RANKL-induced gene expression of c-Fos and NFATc1. C: OA10 inhibited the protein expression level of c-Fos and NFATc1, the gray level of c-Fos and NFATc1 were analyzed and normalized to GAPDH using ImageJ and are presented graphically (bottom) ($^{**}P < 0.01$). And the gray level of phosphorylation of p38 was analyzed and normalized to GAPDH using ImageJ and are presented graphically (bottom) ($^{*}P < 0.05$; $^{**}P < 0.01$).

[Huang et al., 2006; Sharma et al., 2007]. Accordingly, we examined the effects of OA10 on the RANKL-induced regulation of c-Fos and NFATc1 expression. Indeed, our results revealed that c-Fos and NFATc1 mRNA levels were upregulated in response to RANKL. However, gene expression of c-Fos and NFATc1 expression was strongly inhibited by OA10 in both time- and dose-dependent manner (Fig. 5B). Additionally, Western blots analysis further confirmed the suppression of c-Fos and NFATc1 protein level by OA10 (Fig. 5C). Taken together, OA10 inhibited osteoclast formation by suppressing p38 induced c-Fos and NFATc1 expression.

DISCUSSION

Excessive osteoclastic bone resorption is playing a primary role in the development of bone diseases such as osteoporosis and implant failure [Rodan, 2000; Boyce et al., 2012]. Thus, the inhibition of osteoclast differentiation and bone resorption is a viable method for the treatment of these diseases. Here, in this study, we for the first time demonstrated the synthesized novel compound Tert-butyl4-(3-[1H-indole-2-carboxamido]benzoyl)piperazine-1-carboxylate (denoted as OA10) is capable of suppressing osteoclast formation and bone resorption via inhibiting the p38 induced c-fos and NFATc1 expression. Thus, suggesting the synthesis of this compound is potential for the treatment of osteoclast-related bone diseases.

The novel compound OA10 we synthesized is based on Scio 469 (Fig. 1A), a well-studied p38α inhibitor involved in the inhibition of osteoclast differentiation and bone resorption [Vanderkerken et al., 2007]. Some p38α inhibitors such as Pamapimod [Hill et al., 2008], Scio 469 [Vanderkerken et al., 2007], VX 702 [Cohen and Fleischmann, 2010], and PH 797804 [Xing et al., 2012] achieve their high kinase selectivity by positioning ligand side chains in multiple "selectivity hotspots." These hotspots are regions in or in proximity to the ATP-binding site where the amino acid sequence of p38α is distinct from the majority of other human kinases. Therefore, engaging this region of the protein with the appropriate ligand interaction results in significant selectivity gain. Met109, Gly110, and Thr106 are very important amino acid residues in hinge region, largely determines the inhibitor binding and ATP-binding pocket close degree [Wrobleski et al., 2013]. Potent p38α inhibitors can produce hydrogen-bonding interactions with amino acids Met109, Gly110; they were although able to occupy the back hydrophobic pocket. Based on these binding sites, we use Scio469 as a lead compound to design a class of novel p38α protein kinase inhibitors. In Part 1 section, we introduce the heterocyclic ring, hope as well as the formation of new hydrogen bonds and hydrophobic pocket formed after a certain van der Waals interaction, the indole ring is first introduced. In Part 2 section, we reserve the amide bond, and hope to form hydrogen bonds with Met109 and Gly110 thereby enhancing compounds targeting selective; In Part 3, a piperazine group is introduced to insert into the hydrophobic pocket (Fig. 1B).

Not surprisingly, OA10 revealed inhibitory effect on osteoclastogenesis in a dose-dependent manner without major cell cytotoxicity (Fig. 2A and B). Furthermore, the inhibition of osteoclast differentiation was confirmed by evaluating the mRNA expression level of osteoclastic-specific genes including CTR, CTSK, and TRAP. Furthermore, we have also demonstrated that osteoclastic bone resorption function was also suppressed in the presence of OA10 (Fig. 4A and B).

To elucidate involvement of signal transduction and the mechanisms underlying the inhibition of RANKL-induced osteoclast differentiation by OA10, we examined the effect of OA10 on RANKL-induced signaling cascades such as p38, JNK, and IkBα. Our data show OA10 inhibited the phosphorylation of p38, a key step during RANKL-induced osteoclastogenesis [Matsumoto et al., 2000]. Previous studies have demonstrated that activation of p38 is a key step in bone destruction while the inhibition of p38 activity with SB203580 (a specific p38 pathway inhibitor) reduced osteoclast formation and bone destruction [Huang et al., 2006; Zwerina et al., 2006]. Similarly, other compounds include fisetin [Choi et al., 2012], ethyl acetate fraction [Lee et al., 2010], indoxyl sulfate [Mozar et al., 2012], and plant limonoid 7-oxo-deacetoxygedunin [Wisutsitthiwong et al., 2011] are also capable of inhibiting p38 activation and suppressing osteoclast formation. Thus, our study synthesized a novel compound that can inhibit p38 phosphorylation.

RANKL-induced activation of p38 MAP kinase further induce the expression of osteoclast-specific genes, including c-Fos and NFATc1 [Huang et al., 2006], two crucial transcriptional factors in osteoclast formation [Takayanagi et al., 2002; Teitelbaum, 2004]. c-Fos is a major component of the transcription factor AP-1, and can induce NFATC1 to regulate osteoclasts formation by binding to the promoter region of NFATc1, a master regulator of osteoclastogenesis [Lucas et al., 1998; Takayanagi et al., 2002]. In our study, we found the suppression of p38 phosphorylation by OA10 subsequently suppressed c-fos and NFATc1 in a dose-dependent manner, leading to the inhibition of osteoclast formation and bone resorption.

In summary, our result demonstrated that Tert-butyl 4-(3-[1H-indole-2-carboxamido]benzoyl)piperazine-1-carboxylate (OA10) can suppress osteoclastogenesis and reduce bone resorption. The inhibitory effect of OA10 in osteoclastogenesis and bone resorption is mediated by the attenuation of p38 activation. Scio-469 is a specific p38alpha mitogen-activated protein kinase inhibitor for osteolytic diseases and rheumatoid arthritis. Admittedly, this is a potential compound for the treatment of osteoclast-related diseases. However, this is still not a clinically widely used compound compared with denosumab or bisphosphonates. Therefore, our aim was to synthesize new compound that has potential in treating osteoclast diseases. Here, we synthesize a new compound (OA10) which inhibited osteoclast formation by suppressing p38 induced c-Fos and NFATc1 expression. This is the first time we synthesized OA10 based on Scio-469 and certified that OA10 inhibited osteoclast formation through p38-c-Fos-NFATc1 pathway. Further experiments comparing the effect of OA10 and Scio-469 for the treatment of osteolytic diseases in vitro and in vivo are required.

ACKNOWLEDGMENTS

This work was supported by grants from National Nature Science Foundation of China (81101338 and 81125013) (to D.S. and Q.J.), the National Health and Medical Research Council (1010420, J.X. and M.H.Z.), Shanghai Municipal Education Commission (13YZ031), and the National Natural Science Foundation for the Youth of China (No. 81201364).

REFERENCES

Boyce BF, Xing L, Franzoso G, Siebenlist U. 1999. Required and nonessential functions of nuclear factor-kappa B in bone cells. Bone 25:137–139.

Boyce BF, Rosenberg E, de Papp AE, le Duong T. 2012. The osteoclast, bone remodelling and treatment of metabolic bone disease. Eur J Clin Invest 42: 1332–1341.

Chambers TJ. 2000. Regulation of the differentiation and function of osteoclasts. J Pathol 192:4–13.

Choi SW, Son YJ, Yun JM, Kim SH. 2012. Fisetin inhibits osteoclast differentiation via downregulation of p38 and c-Fos-NFATc1 signaling pathways. Evid Based Complement Alternat Med 2012:810563.

Cohen S, Fleischmann R. 2010. Kinase inhibitors: a new approach to rheumatoid arthritis treatment. Curr Opin Rheumatol 22:330–335.

Feng H, Cheng T, Steer JH, Joyce DA, Pavlos NJ, Leong C, Kular J, Liu J, Feng X, Zheng MH, Xu J. 2009. Myocyte enhancer factor 2 and microphthalmia-associated transcription factor cooperate with NFATc1 to transactivate the V-ATPase d2 promoter during RANKL-induced osteoclastogenesis. J Biol Chem 284:14667–14676.

Gingery A, Bradley E, Shaw A, Oursler MJ. 2003. Phosphatidylinositol 3-kinase coordinately activates the MEK/ERK and AKT/NFkappaB pathways to maintain osteoclast survival. J Cell Biochem 89:165–179.

Grigoriadis AE, Wang ZQ, Cecchini MG, Hofstetter W, Felix R, Fleisch HA, Wagner EF. 1994. c-Fos: a key regulator of osteoclast-macrophage lineage determination and bone remodeling. Science 266:443–448.

Hill RJ, Dabbagh K, Phippard D, Li C, Suttmann RT, Welch M, Papp E, Song KW, Chang KC, Leaffer D, Kim YN, Roberts RT, Zabka TS, Aud D, Dal Porto J, Manning AM, Peng SL, Goldstein DM, Wong BR. 2008. Pamapimod, a novel p38 mitogen-activated protein kinase inhibitor: preclinical analysis of efficacy and selectivity. J Pharmacol Exp Ther 327:610–619.

Huang H, Chang EJ, Ryu J, Lee ZH, Lee Y, Kim HH. 2006. Induction of c-Fos and NFATc1 during RANKL-stimulated osteoclast differentiation is mediated by the p38 signaling pathway. Biochem Biophys Res Commun 351:99–105.

Izawa T, Zou W, Chappel JC, Ashley JW, Feng X, Teitelbaum SL. 2012. c-Src links a RANK/alphavbeta3 integrin complex to the osteoclast cytoskeleton. Mol Cell Biol 32:2943–2953.

Lee EG, Yun HJ, Lee SI, Yoo WH. 2010. Ethyl acetate fraction from *Cudrania tricuspidata* inhibits IL-1beta-stimulated osteoclast differentiation through downregulation of MAPKs, c-Fos and NFATc1. Korean J Intern Med 25: 93–100.

Li H, Zhai Z, Liu G, Tang T, Lin Z, Zheng M, Qin A, Dai K. 2013. Sanguinarine inhibits osteoclast formation and bone resorption via suppressing RANKL-induced activation of NF-kappaB and ERK signaling pathways. Biochem Biophys Res Commun 430:951–956.

Lucas JJ, Yamamoto A, Scearce-Levie K, Saudou F, Hen R. 1998. Absence of fenfluramine-induced anorexia and reduced c-Fos induction in the hypothalamus and central amygdaloid complex of serotonin 1B receptor knock-out mice. J Neurosci 18:5537–5544.

Mansky KC, Sankar U, Han J, Ostrowski MC. 2002. Microphthalmia transcription factor is a target of the p38 MAPK pathway in response to receptor activator of NF-kappa B ligand signaling. J Biol Chem 277:11077–11083.

Matsumoto M, Sudo T, Maruyama M, Osada H, Tsujimoto M. 2000. Activation of p38 mitogen-activated protein kinase is crucial in osteoclastogenesis induced by tumor necrosis factor. FEBS Lett 486:23–28.

Matsuo K, Galson DL, Zhao C, Peng L, Laplace C, Wang KZ, Bachler MA, Amano H, Aburatani H, Ishikawa H, Wagner EF. 2004. Nuclear factor of activated T-cells (NFAT) rescues osteoclastogenesis in precursors lacking c-Fos. J Biol Chem 279:26475–26480.

Mozar A, Louvet L, Godin C, Mentaverri R, Brazier M, Kamel S, Massy ZA. 2012. Indoxyl sulphate inhibits osteoclast differentiation and function. Nephrol Dial Transpl 27:2176–2181.

Nakashima T, Hayashi M, Fukunaga T, Kurata K, Oh-Hora M, Feng JQ, Bonewald LF, Kodama T, Wutz A, Wagner EF, Penninger JM, Takayanagi H. 2011. Evidence for osteocyte regulation of bone homeostasis through RANKL expression. Nat Med 17:1231–1234.

Qin A, Cheng TS, Lin Z, Pavlos NJ, Jiang Q, Xu J, Dai KR, Zheng MH. 2011. Versatile roles of V-ATPases accessory subunit Ac45 in osteoclast formation and function. PLoS ONE 6:4.

Qin A, Cheng TS, Lin Z, Cao L, Chim SM, Pavlos NJ, Xu J, Zheng MH, Dai KR. 2012. Prevention of wear particle-induced osteolysis by a novel V-ATPase inhibitor saliphenylhalamide through inhibition of osteoclast bone resorption. PLoS ONE 7:11.

Rodan GA. 2000. Therapeutic approaches to bone diseases. Science 289:1508–1514.

Sharma SM, Bronisz A, Hu R, Patel K, Mansky KC, Sif S, Ostrowski MC. 2007. MITF and PU.1 recruit p38 MAPK and NFATc1 to target genes during osteoclast differentiation. J Biol Chem 282:15921–15929.

Simic P, Culej JB, Orlic I, Grgurevic L, Draca N, Spaventi R, Vukicevic S. 2006. Systemically administered bone morphogenetic protein-6 restores bone in aged ovariectomized rats by increasing bone formation and suppressing bone resorption. J Biol Chem 281:25509–25521.

Takayanagi H, Kim S, Koga T, Nishina H, Isshiki M, Yoshida H, Saiura A, Isobe M, Yokochi T, Inoue J, Wagner EF, Mak TW, Kodama T, Taniguchi T. 2002. Induction and activation of the transcription factor NFATc1 (NFAT2) integrate RANKL signaling in terminal differentiation of osteoclasts. Dev Cell 3:889–901.

Tanos T, Marinissen MJ, Leskow FC, Hochbaum D, Martinetto H, Gutkind JS, Coso OA. 2005. Phosphorylation of c-Fos by members of the p38 MAPK family. Role in the AP-1 response to UV light. J Biol Chem 280:18842–18852.

Teitelbaum SL. 2000. Bone resorption by osteoclasts. Science 289:1504–1508.

Teitelbaum SL. 2004. RANKing c-Jun in osteoclast development. J Clin Invest 114:463–465.

Vanderkerken K, Medicherla S, Coulton L, De Raeve H, Willems A, Lawson M, Van Camp B, Protter AA, Higgins LS, Menu E, Croucher PI. 2007. Inhibition of p38alpha mitogen-activated protein kinase prevents the development of osteolytic bone disease, reduces tumor burden, and increases survival in murine models of multiple myeloma. Cancer Res 67:4572–4577.

Wisutsitthiwong C, Buranaruk C, Pudhom K, Palaga T. 2011. The plant limonoid 7-oxo-deacetoxygedunin inhibits RANKL-induced osteoclastogenesis by suppressing activation of the NF-kappaB and MAPK pathways. Biochem Biophys Res Commun 415:361–366.

Wrobleski ST, Lin S, Murali Dhar TG, Dyckman AJ, Li T, Pitt S, Zhang R, Fan Y, Doweyko AM, Tokarski JS, Kish KF, Kiefer SE, Sack JS, Newitt JA, Witmer MR, McKinnon M, Barrish JC, Dodd JH, Schieven GL, Leftheris K. 2013. The identification of novel p38alpha isoform selective kinase inhibitors having an unprecedented p38alpha binding mode. Bioorg Med Chem Lett 23:4120–4126.

Xing L, Devadas B, Devraj RV, Selness SR, Shieh H, Walker JK, Mao M, Messing D, Samas B, Yang JZ, Anderson GD, Webb EG, Monahan JB. 2012. Discovery and characterization of atropisomer PH-797804, a p38 MAP kinase inhibitor, as a clinical drug candidate. ChemMedChem 7:273–280.

Xiong J, Onal M, Jilka RL, Weinstein RS, Manolagas SC, O′Brien CA. 2011. Matrix-embedded cells control osteoclast formation. Nat Med 17:1235–1241.

Zwerina J, Hayer S, Redlich K, Bobacz K, Kollias G, Smolen JS, Schett G. 2006. Activation of p38 MAPK is a key step in tumor necrosis factor-mediated inflammatory bone destruction. Arthritis Rheum 54:463–472.